2010-08

Initial Maintenance of Tropical Cyclone Size in the Western North Pacific

Lee, Cheng-Shang

Initial Maintenance of Tropical Cyclone Size in the Western North Pacific

CHENG-SHANG LEE

Department of Atmospheric Sciences, National Taiwan University, and Typhoon and Flood Research Institute, National Applied Research Laboratories, Taipei, Taiwan

KEVIN K. W. CHEUNG

Climate Futures Research Centre, and Department of Environment and Geography, Macquarie University, Sydney, Australia

WEI-TING FANG

Department of Atmospheric Sciences, National Taiwan University, Taipei, Taiwan

RUSSELL L. ELSBERRY

Department of Meteorology, Naval Postgraduate School, Monterey, California

(Manuscript received 31 March 2009, in final form 18 February 2010)

ABSTRACT

A tropical cyclone (TC) size parameter, which is defined here as the radius of 15 m s^{-1} near-surface wind speed (R15), is calculated for 145 TCs in the western North Pacific during 2000–05 based on QuikSCAT oceanic winds. For the 73 TCs that intensified to typhoon intensity during their lifetimes, the 33% and 67% respective percentiles of R15 at tropical storm intensity and at typhoon intensity are used to categorize small, medium, and large TCs. Whereas many of the small TCs form from an easterly wave synoptic pattern, the monsoon-related formation patterns are favorable for forming medium to large TCs. Most of these 73 TCs stay in the same size category during intensification, which implies specific physical mechanisms for maintaining TC size in the basin. The 18 persistently large TCs from the tropical storm to the typhoon stage mostly have northwestward or north-northwestward tracks, while the 16 persistently small TCs either move westward–northwestward in lower latitudes or develop at higher latitudes with various track types. For the large TCs, strong low-level southwesterly winds exist in the outer core region south of the TC center throughout the intensification period. The small TCs are more influenced by the subtropical high during intensification. The conclusion is that it is the low-level environment that determines the difference between large and small size storms during the early intensification period in the western North Pacific.

1. Introduction

The size of a tropical cyclone (TC) is a significant structure parameter not only because it roughly indicates the area in which much of the cyclone kinetic energy that may cause damages is found (Powell and Reinhold 2007; Maclay et al. 2008) but also because the motion of a TC is affected by size. The latter is due to the fact that the actual motion of a TC deviates from the large-scale steering flow by what is known as beta-effect propagation (BEP), and it has been shown in previous studies that the magnitude of the BEP vector depends sensitively on the outer (>300 km) wind structure (Holland 1983; Fiorino and Elsberry 1989; Carr and Elsberry 1997). No universal definition of TC size exists. When few observations of surface wind were available, TC size was often defined as the radius of the outer closed isobar (ROCI) from the surface weather maps (Brand 1972; Merrill 1984). The availability of remote sensing techniques such as geostationary infrared (IR) satellite imageries, the Special Sensor Microwave Imager (SSM/I), and the Advanced Microwave Sounding Unit (AMSU) now allow a range of structure parameters, including the radius of maximum

Corresponding author address: Kevin K. W. Cheung, Department of Environment and Geography, Macquarie University, Sydney, NSW 2109, Australia.
E-mail: kcheung@els.mq.edu.au

DOI: 10.1175/2010MWR3023.1

wind (RMW), to be derived. [Results for the radius of maximum wind were found for winds of 34 kt (17.5 m s^{-1}), 50 kt (25.7 m s^{-1}), and 64 kt (32.9 m s^{-1}) by Mueller et al. (2006), Kossin et al. (2007, IR-based), and Demuth et al. (2004, 2006) and Bessho et al. (2006, both AMSU-based)]. In addition, algorithms have been developed to obtain both wind speed and direction from the early European Remote Sensing (ERS)-½ scatterometer (Quilfen et al. 1998), the National Aeronautics and Space Administration (NASA) Scatterometer (NSCAT; Polito et al. 2000), the QuikSCAT satellite (Hoffman et al. 2003), and the Advanced Scatterometer (ASCAT) from the European Organisation for the Exploitation of Meteorological Satellites (EUMETSAT).

Whatever definition is assigned for TC size, it is a dynamical parameter that changes in various ways during the evolution of the TC. Some studies have focused on the dynamics of size change, its associated climatology, and relationship with other synoptic systems. For example, Merrill (1984) analyzed the angular momentum budget of TCs in the western North Pacific (WNP) with increasing ROCI and intensity and found that a large portion of the angular momentum increase is associated with a ROCI increase rather than intensification. Merrill then concluded that the dynamical processes for size change are different from those for intensification, which is consistent with the low statistical correlation between size and intensity changes (Weatherford and Gray 1988a,b). That is, Weatherford and Gray (1988a,b) found that strengthening of winds in the inner core (0°–1° latitude) and outer core (1°–2.5° latitude) are quite independent, and hence structure changes in the two regions are associated with different dynamical processes.

It is also known that TC size varies seasonally and has a latitudinal dependence. Kimball and Mulekar (2004) and Liu and Chan (1999) indicate that TC size is largest in September and October for Atlantic hurricanes, and particularly in October for western North Pacific TCs. A general relationship of increasing TC size with latitude is identified in studies such as Weatherford and Gray (1988a,b) and may be due to interaction with midlatitude synoptic systems. In performing multiple regression analyses of TC structure parameters, Mueller et al. (2006) and Kossin et al. (2007) both identified that latitude is one of the necessary predictors. Similarly, latitude is also one of the factors used in developing the climatology-persistence wind radii model in Knaff et al. (2007). The dependence on latitude as shown in these studies is in accord with the TC wind structure model in Carr and Elsberry (1997), which shows that the increase of the Coriolis parameter with latitude will increase the slope of the outer core wind profile and thus will affect the size of a TC.

Liu and Chan (2002) show that large TCs in the WNP are usually accompanied by a southwesterly surge or occur in late season when both the northeasterly winter monsoonal flow and southeasterlies associated with the subtropical ridge increase the outer core wind speed. In contrast, small TCs are usually embedded in the strong easterly trades of the subtropical ridge or on the eastern periphery of the monsoon gyre. Other factors that may affect TC size include climatological ones such as speed of motion, intensity, and intensification rate and synoptic factors such as vertical wind shear.

It is obviously important that forecasters have the techniques to skillfully predict future structure changes of TCs to issue accurate warnings of gale-force winds. However, improved understanding of structure change depends strongly on the availability of reliable surface wind datasets. For Atlantic hurricanes, the observation-based H*Wind dataset from the Hurricane Wind Analysis System is available for analysis (Powell et al. 1998; Powell and Reinhold 2007; Elsberry and Stenger 2008). For WNP TCs, only satellite-retrieved winds are available. Fortunately, some of these remote sensing datasets have been accumulated for years such that an adequate number of TC cases can be analyzed.

Whereas most of the previous studies on TC size have concentrated on how internal processes and interactions with external systems determine size or lead to size change, the focus of this study is different. Rather than concentrating on how size changes, the focus is on how TC size is maintained during its initial evolution (i.e., why do most storms maintain their size during the intensification period?). For this purpose, size for each TC is determined from the early development stage [tropical storm (TS) intensity] until the mature stage [reaching typhoon (TY) intensity] with respect to a sophisticated synoptic pattern classification scheme in which differences in the origin of large and small TCs are revealed. In particular, a synoptic pedigree of TC size during the early intensification period is established in a more quantitative sense compared with discussions in some previous studies.

The organization of this paper is as follows: Data sources and the methodology to determine TC size in this study are given in the following section. In section 3, variability of the size parameter with respect to timing within a season and synoptic patterns is documented, and then several size categories are defined. Section 4 is devoted to comparing the synoptic situation and convection characteristics of persistently large and small TCs during their intensification periods. Finally, a summary and some concluding remarks comparing these results with related studies are presented in section 5.

2. Determination of TC size from QuikSCAT oceanic winds

a. Data sources

Oceanic winds retrieved from the QuikSCAT satellite during the 2000–05 seasons in the WNP are obtained. The QuikSCAT swath width is about 1800 km, the horizontal resolution is about 25 km, and the ascending and descending swaths for a particular location are about 12 h apart. Ebuchi et al. (2002) and Pickett et al. (2003) validated QuikSCAT winds with buoy observations that are remote from coasts. If winds weaker than 3 m s^{-1} and those contaminated by rainfall are ignored, the root-mean-square error is about 1.0 m s^{-1} for wind speed and about 15°–20° for wind direction, which shows the applicability of the QuikSCAT winds for examination of the TC surface wind distribution.

Best tracks of the TCs are obtained from the Joint Typhoon Warning Center (JTWC), which consist of 6-hourly positions of the 145 TCs that occurred in the basin during 2000–05. The synoptic environment associated with these TCs is examined using the National Centers for Environmental Prediction (NCEP)–Department of Energy (DOE) Reanalysis 2 dataset (Kanamitsu et al. 2002) with 2.5° latitude–longitude horizontal resolution and 6-h temporal resolution. In addition, convective patterns within these TCs are monitored by the hourly imagery from the *Geostationary Meteorological Satellite 5* (*GMS-5*) and *Geostationary Operational Environmental Satellite 9* (*GOES-9*) infrared channel-1 (IR1) cloud-top temperatures with 5-km resolution and spatial coverage of 20°S–70°N, 70°–160°E. The satellite imagery is obtained from a digital archive at the Kochi University of Japan.

b. Determination of R15

Following Frank and Gray (1980) and Cocks and Gray (2002), the radius of 15 m s^{-1} wind speed (R15) is defined as the TC size in this study. Since the QuikSCAT overpass does not necessarily coincide with the TC best-track positions, the center position at the time of the QuikSCAT winds is obtained by temporal interpolation of the nearest JTWC positions. Then the QuikSCAT wind speed and direction are converted to tangential and radial wind components at grid points in a storm-relative cylindrical coordinate system. The radial grid increment is 0.1° latitude, and wind components are calculated for every azimuthal degree (i.e., 360 data points on a circle). The azimuthal-average tangential wind profile of a TC (Fig. 1a) at the time of the QuikSCAT swath is calculated and then R15 is the radius at which the total wind speed equals 15 m s^{-1} outward from its maximum

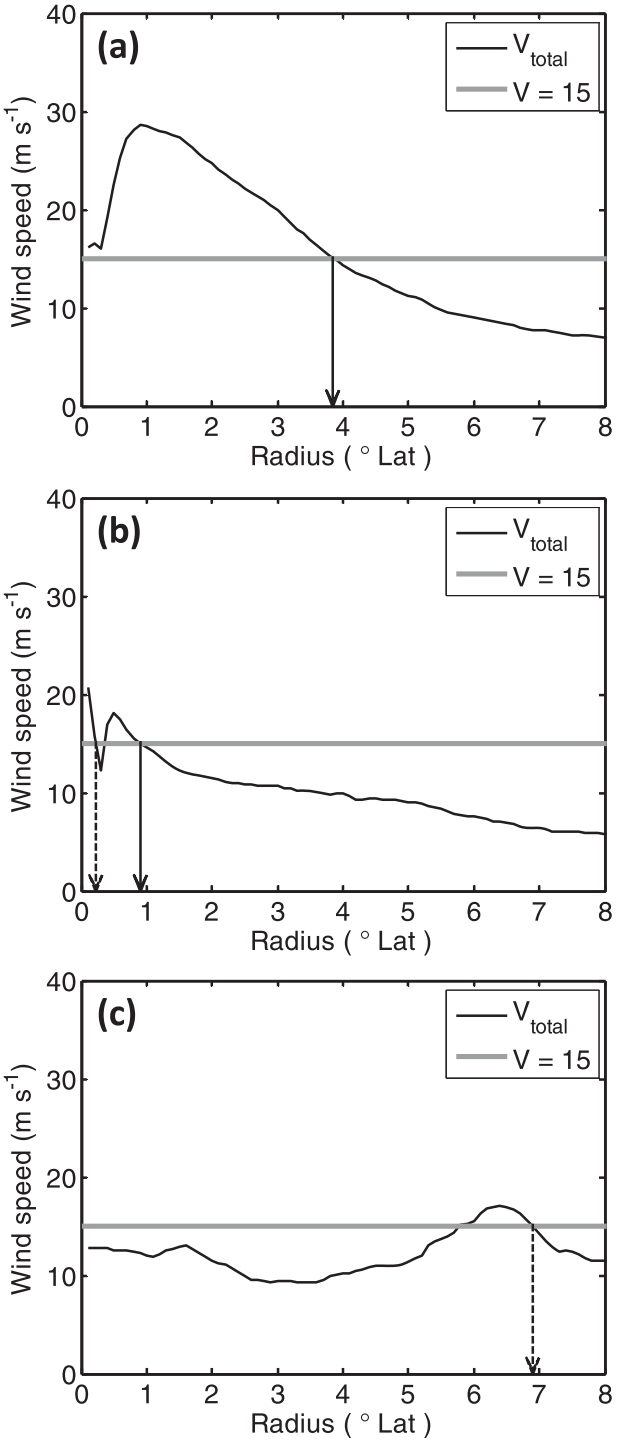

FIG. 1. Examples of R15 estimates (dashed vertical lines) from QuikSCAT oceanic winds for (a) Typhoon Aere at 2136 UTC 22 Aug 2004, (b) Typhoon Jelawat at 1911 UTC 1 Aug 2000, and (c) Typhoon Kajiki at 2103 UTC 6 Dec 2001.

value near the eyewall. Since all points in these circular grids may not be covered by the QuikSCAT swath, it is required that at least 50% of the grid points be covered by QuikSCAT winds.

In some of the cases, the interpolated TC center position from the JTWC best track is not well matched with the circulation center as depicted in the QuikSCAT oceanic winds, which introduces a second maximum in the radial wind profile. Calculations with idealized Rankine vortices indicate that the induced second maximum is within the original radius of maximum wind, and when the shift in center position is less than the RMW, the wind profile outside the RMW (and hence the R15 estimate) almost remains unchanged. For example, there are two wind maxima in the tangential wind profile of Typhoon Jelawat (2000) in Fig. 1b. The first radius to have a wind speed of 15 m s^{-1} is about 30 km, but by the above arguments the second radius to reach 15 m s^{-1}, which is about 100 km, is the appropriate R15 estimate. Nevertheless, there are only 23 times among all the TC periods at which these kinds of double maxima in radial wind profile occur and they are at various intensities. Thus, the impact on the overall R15 distribution is not substantial. The analysis will exclude TCs below tropical storm intensity (34 kt or 17.5 m s^{-1}) because they may not have an inner core wind speed of 15 m s^{-1} and hence would not possess an R15. This is illustrated in Fig. 1c where the average inner core wind speed is less than 15 m s^{-1} with an outer core wind maximum such that an overestimation of R15 occurs. With these conditions and exclusions, the dataset consists of 994 values of R15.

Tests excluding those QuikSCAT winds that are labeled as rain contaminated (Weissman et al. 2002) resulted in little changes in the R15 estimates (not shown). The likely explanation is that although exclusion of the potentially contaminated winds improves the overall data quality, the impact on the TC size estimate is minimal because of the averaging of large numbers of winds in each azimuth. Including all QuikSCAT data also increases the number of R15 values that qualify for subsequent analysis by meeting the 50% data coverage requirement.

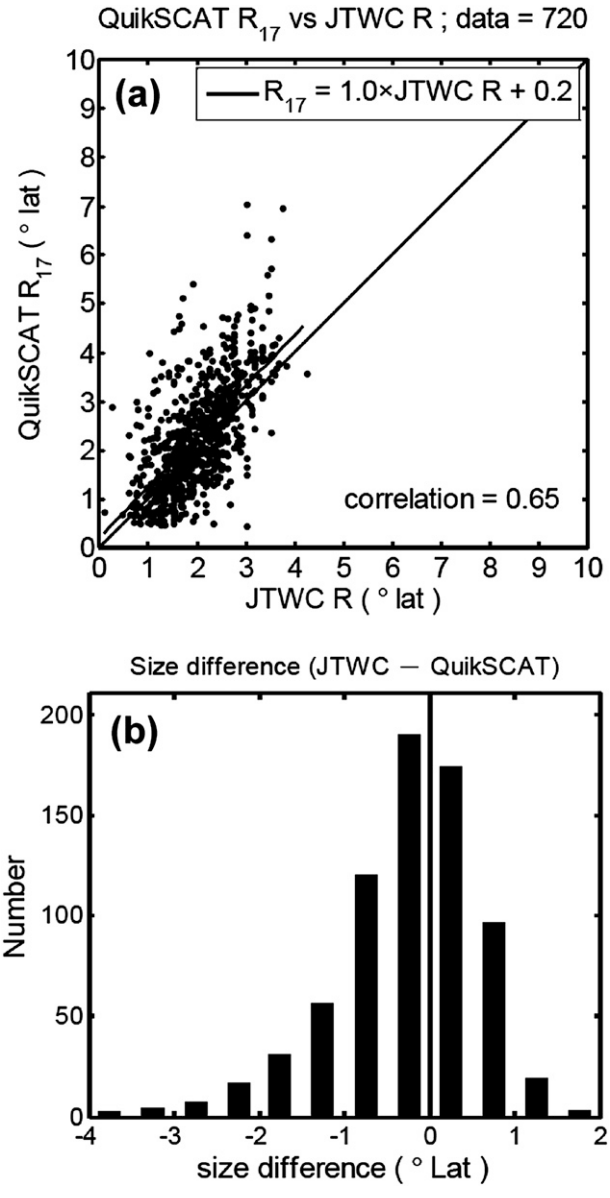

FIG. 2. (a) Scatterplot and regression line of radius with 17.5 m s^{-1} wind speed as determined by QuikSCAT oceanic winds (QS-R17) against the average 34-kt radius in the JTWC best-track file. (b) Histogram of the difference between the two radii (JTWC minus QS-R17) with a 0.5° lat bin size.

c. *QuikSCAT-based size versus JTWC size*

Starting from the 2001 TC season, the JTWC best-track file includes estimates of 34-kt (17.5 m s^{-1}) winds in the four quadrants. To compare the TC size inferred from QuikSCAT data with these JTWC estimates, radii of 17.5 m s^{-1} azimuthally averaged wind (QS-R17) are also calculated based on the same procedure used for obtaining R15. The nonzero JTWC 34-kt wind estimates in the four quadrants at the nearest 6-h synoptic time to the QS-R17 are also averaged to get a single size parameter. The correlation coefficient between these two size estimates for 720 cases during 2001–05 is 0.65 with a p value much lower than 0.05 (i.e., the correlation is statistical significant; Fig. 2a). The positive 0.2° latitude intercept of the regression line implies that QS-R17 is generally larger than the JTWC estimate, which is consistent with the negatively skewed distribution of the difference of the JTWC estimate from QS-R17 in Fig. 2b. Usually the operational size estimate from JTWC is

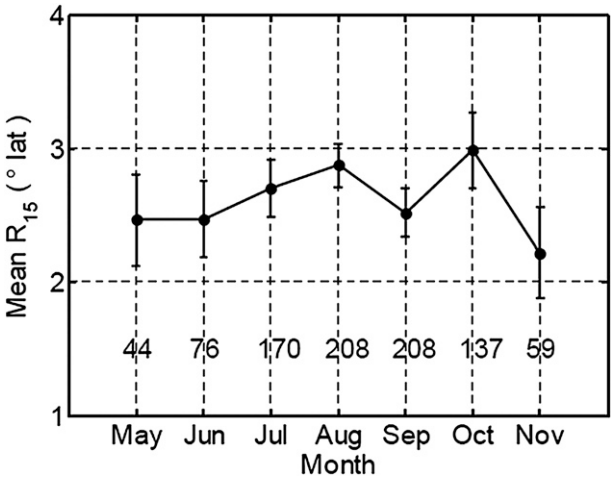

FIG. 3. Monthly average value of R15. Error bars indicate 5% and 95% percentiles, and underneath each data point is the number of cases for that month.

rather subjective and dependent on in-house climatologies and analysis methods (Knaff et al. 2007). Nevertheless, given that in 77% of the cases this size difference is within 1° of latitude, the application of climatology and persistence for size estimate in the JTWC should be justified. However, in some occasions the JTWC adjusts the outer core winds according to the surface pressure gradient or separate synoptic wind radii from vortex wind radii in TC advisories. Sometimes, the eye sizes are adjusted according to passive microwave imageries (Lander et al. 2006), which will affect the radial wind profile used for size estimation and lead to larger deviations of the size parameter from the QuikSCAT estimates.

3. Size variability and formation patterns

a. R15 seasonality

Monthly average R15 values (Fig. 3) have little seasonal variability, with all months except November having values between 2.5° and 3.0° latitude. These average values of R15 are consistent with the average radius of 34-kt (17.5 m s^{-1}) winds, which is 115 nautical miles or 1.9° latitude, identified in Knaff et al. (2007). Brand (1972), Merrill (1984), Liu and Chan (1999), and Yuan et al. (2007) also found that TC size has a slight increasing trend from the beginning of the season, reaches a maximum in October, and then decreases in the late season (November and December). The relatively small value of the average R15 in September is in contrast with the TC size climatology established based on a 28-yr (1977–2004) dataset in Yuan et al. (2007). When R15 values in September for individual years are examined, it is found that those in 2001 and 2002 are very small, and it is believed the shorter study period here makes the results more sensitive to the extreme values. The small R15s may be due to the fact that the years 2001 and 2002 have decaying La Niña and starting El Niño conditions, respectively, and the TC formation positions are more in the eastern part of the basin (Chan and Yip 2003). According to the R15 spatial distribution in Yuan et al. (2007), more small R15 values are found in the eastern WNP. The small size of the late-season (November and December) TCs is attributed to formation at lower latitudes due to southward migration of the monsoon shear line (Cheung 2004). These late-season storms have shorter lifetimes and do not intensify as much as the summer storms. Although these late-season storms stay in the low latitudes, they do not interact as much with subtropical systems or regions with large vertical wind shear that are favorable for size increase.

b. R15 dependence on intensity and latitude

Weak dependence of R15 with TC intensity (correlation coefficient of 0.3) is found, which agrees very well with Merrill (1984), who found a correlation coefficient of 0.28 for North Atlantic storms. Merrill found a higher percentage of large hurricanes (as measured by ROCI) at about 30°N, where lower sea surface temperatures and increasing vertical wind shear would be expected to lead to intensity decrease. Although a similar tendency might be inferred from Fig. 4a that shows most large TCs are moving northwestward to higher latitudes, some small storms also form at higher latitudes in the WNP (Fig. 4b). This is why a large variation in latitude is found for each of the R15 values identified (Fig. 5). Considering that most TCs weaken when they are traveling to higher latitudes and that a weak relationship exists between R15 and latitude, a low correlation of size and intensity is expected.

c. Small, medium, and large TCs

The focus in this section is on TC size evolution during the intensification to at least typhoon stage (64 kt or 32.9 m s^{-1}). Thus, the sample is limited to the 73 storms that intensified to typhoon during their lifetimes. Azimuthal average R15 values at the first sampled time period during the tropical storm (34 kt or 17.5 m s^{-1}) stage are designated as R15-TS and during the typhoon stage as R15-TY. Then these 73 TC storms are categorized as small, medium, and large according to the 33% and 67% percentiles within the R15-TS and R15-TY distributions. These tercile values are 1.1° and 1.8° latitude at the TS stage and 1.8° and 2.6° latitude at the TY stage (Table 1). Coincidentally, 24 small, 24 medium,

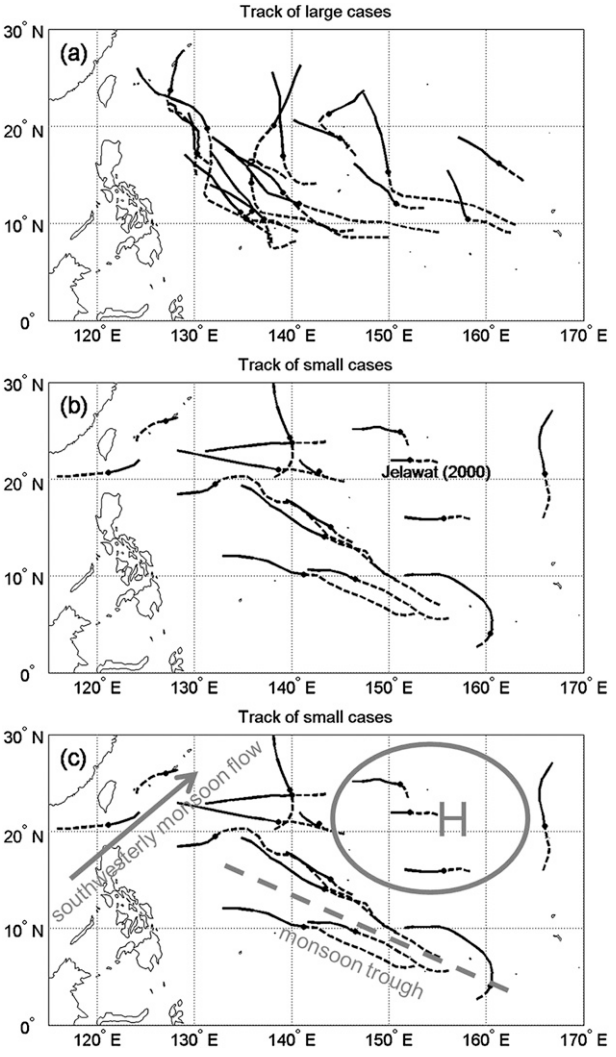

FIG. 4. Best tracks of the (a) 18 persistently large and (b) 16 persistently small TCs in Table 2, with dashed lines representing the pre-TS stage and solid lines the TS-to-TY stage. (c) As in (b), but with illustrations of the subtropical high, monsoon trough, and southwesterly monsoon flow.

and 25 large cases are found in both the TS and TY stages. The 0.7° (0.8°) latitude increase in R15 for the threshold value of small (large) typhoon versus a small (large) tropical storm in Table 1 indicates an overall spreading toward higher values in the R15 distribution.

The key focus in this section is the size change during the early stage intensification of these 73 TCs. First, the systematic increases in the boundaries of the R15 size categories (e.g., 1.1° latitude for TS but 1.8° latitude for TY, and similarly for the medium and large categories) during intensification from tropical storm to typhoon in Table 1 implies that a natural mode of spinup of the vortex may be the maintenance of the same radial profile of the tangential wind as the intensity increases (see

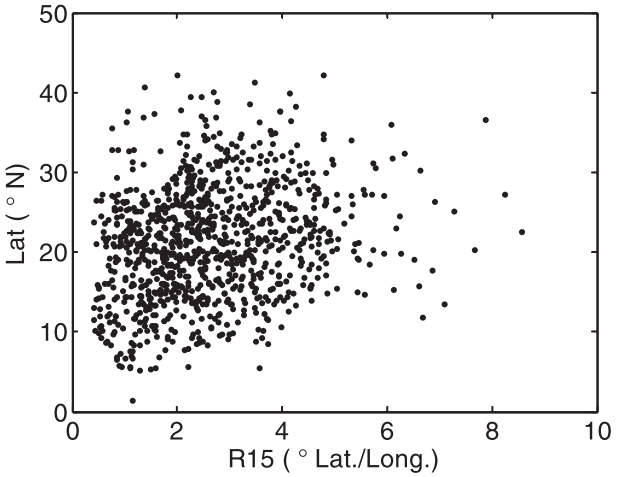

FIG. 5. Scatterplot of latitude against the corresponding R15 value for all the 994 data points from the 145 TCs.

Fig. 2 in Carr and Elsberry 1997). That is, a typical tangential wind v profile for a mature tropical cyclone is a modified Rankine vortex,

$$vr^x = \text{constant}, \tag{1}$$

where r is the radius from the center, $v(r)$ the radial variation of the tangential wind, and x the exponent controlling the tangential wind profile or rate of decrease of the tangential wind from the radius of maximum wind. If x does not change during the intensification (i.e., the rate of decrease is the same) while the maximum wind speed increases in the core region, the radius r at which 30 kt occurs (i.e., R15) must increase. Carr and Elsberry (1997) also considered the model in which the outer wind profile does not change while the inner vortex spins up, which requires an increase in the exponent x.

Most of tropical storms stay in the same size category when they become typhoons. Specifically, 67% of the small tropical storms remain small, and the corresponding percentages for medium and large tropical storms are 50% and 72%, respectively (Table 1). Examples of the average radial wind profiles of TCs that maintain their size categories are illustrated in Fig. 6 (first two rows). For those 33% of small tropical storms that do increase in size, 21% become medium-size typhoons and only 12% become large typhoons. By contrast, all of the large tropical storms that decreased in size as a typhoon only became medium-sized typhoons (i.e., none became small typhoons). This asymmetry in size evolution occurs because a substantial decrease in the size of a large typhoon would require a mechanism for decreasing the angular momentum of the outer core region, or the near-surface angular momentum would have to be dissipated at a high

TABLE 1. Definitions of small, medium, and large TCs (in ° lat) during the TS stage (first column) and TY stage (first row). Number in parentheses is the number of TC cases in each category. The other table entries are the proportion (percentages in parentheses) of cases that change from one TC size category to another during the intensification from TS to TY, and the diagonal entries (bold) indicate cases with no change in TC size category.

TS/TY	Small [<1.8° (24)]	Medium [1.8°–2.6° (24)]	Large [>2.6° (25)]
Small [<1.1° (24)]	**16/24 (67)**	5/24 (21)	3/24 (12)
Medium [1.1°–1.8° (24)]	8/24 (33)	**12/24 (50)**	4/24 (17)
Large [>1.8° (25)]	0/25 (0)	7/25 (28)	**18/25 (72)**

rate. In the latter case, surface friction would need to have an important role (if no exceptionally large vertical transport occurs). However, TCs are mostly over the ocean during their TS-to-TY intensification stage and an explanation for a sudden increase in surface friction in the outer region is not evident.

Notice that the rare transition from a small tropical storm to a large typhoon requires a large spinup of the outer winds since the R15 must increase from <1.1° to >2.6° latitude. (Fig. 6, bottom row). Interestingly, a medium-size tropical storm that does change size as a typhoon is twice as likely to become a small typhoon (8 out of 24) than a large typhoon (4 of 24). Since a small typhoon has a R15 < 1.8° latitude, and the medium-size tropical storm must have an R15 < 1.8° latitude, this situation means absolutely no increase in outer winds during the intensification. Recall that all of these medium-size tropical storms are all intensifying to become typhoons, so the maintenance or decrease in outer winds cannot be attributed to the storm being in a decay stage. By contrast, a large spinup of the outer winds must occur if a medium-size tropical storm is to become a large typhoon, which requires a R15 > 2.6° latitude.

When the values of x in Eq. (1) are explicitly calculated for the radial wind profiles in the 73 TCs, it is found that in 64% of them x indeed increases during intensification from the TS to TY stage. In the categories where TCs maintain their sizes during intensification (i.e., the small–small, medium–medium, and large–large entries in Table 1), the percentages of cases with increased x values are 63%, 67%, and 56%, respectively. While these percentages are consistent with the findings in Demuth et al. (2004, 2006) and Knaff et al. (2007), about 40% of all the TC cases with no change or decreasing exponent x implies that both structure change models considered in Carr and Elsberry (1997) apply to the TCs that maintain their size categories as they intensify to a similar extent.

In summary, the R15 values for TCs in the WNP tend to remain in the same size category during their intensification from TS to TY. An implication of this tendency is that physical mechanisms have to be present to maintain the size of large TSs and to keep the R15 small for small TSs (i.e., to inhibit significant strengthening of outer core winds). Before these physical mechanisms are explored, it is of interest to examine the origins of small and large TCs.

d. R15 and synoptic patterns at formation

Lee et al. (2008) identified six synoptic patterns for TC formation in the WNP based on the low-level wind flow and surge direction: easterly wave (EW), northeasterly flow (NE), coexistence of northeasterly and southwesterly flow (NE–SW), southwesterly flow (SW), monsoon confluence (MC), and monsoon shear (MS). Readers are referred to Lee et al. (2008) for detailed definitions and methodology for identifying the six patterns. This synoptic pattern classification is applied to the TC cases in this study for which R15-TS can be determined with QuikSCAT data during their formation (Fig. 7). In the monsoon-related patterns (MC, MS, SW, and NE–SW), formation of medium to large tropical storms is favored. In particular, strong southwesterly winds are a common ingredient in the MC, SW, and NE–SW synoptic patterns. The MS pattern has strong easterlies and westerlies (>5 m s^{-1}) to the north and south of the depression that also contribute to strong winds in the outer core region, which is somewhat favorable for formation of large tropical storms. Most of the tropical storm formations associated with the EW pattern are either small or medium in size, which is consistent with the finding in Ritchie and Holland (1999) and Lee et al. (2008) that convection and possible mesoscale convective systems in the EW-type formations are mostly concentrated within a small radius (about 1°–2° latitude) from the system center. Since these episodes of convection tend to be confined to an area of low-level vorticity near the center, formation of a smaller-size tropical storm is favored.

4. Large versus small TCs

a. Tracks

Since not all the 145 TCs during 2000–05 intensified to typhoon stage and R15-TS cannot be determined for some cases because of the unavailability of QuikSCAT

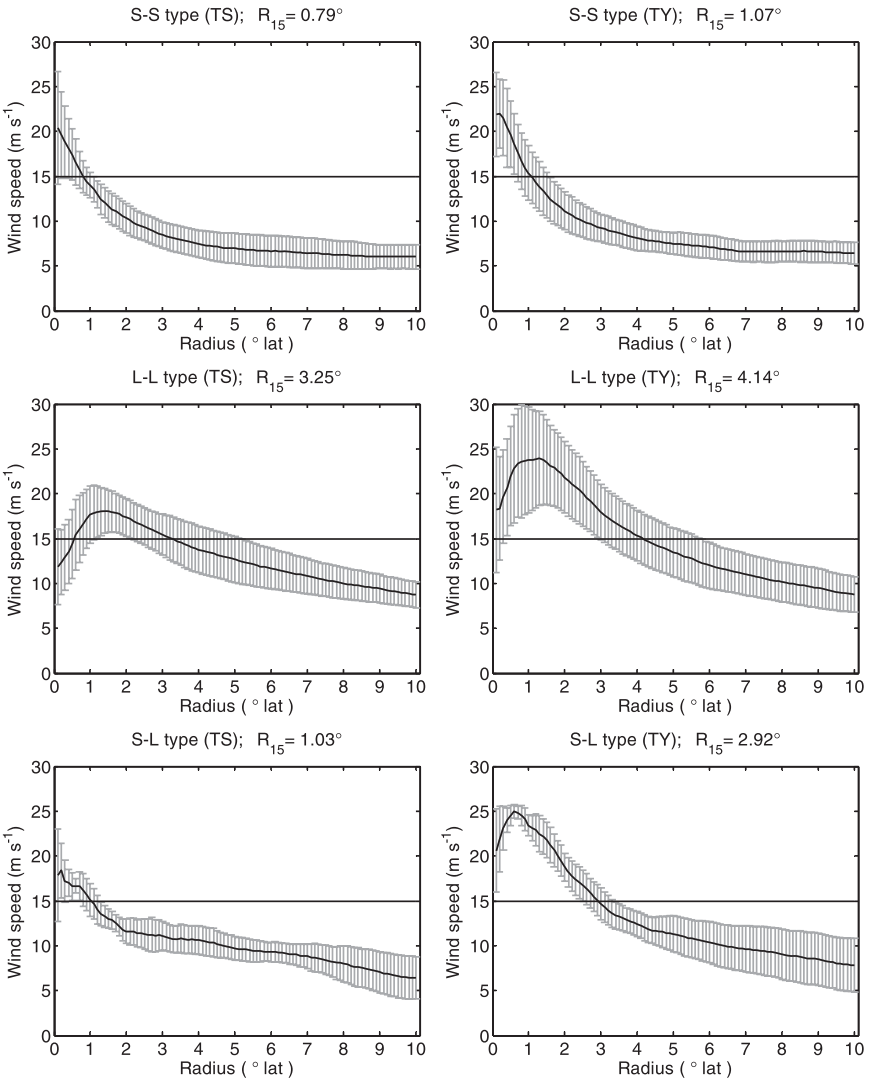

FIG. 6. Average radial wind profiles of TCs at the (left) TS and (right) TY stage that stay in the (top) small and (middle) large size categories and (bottom) that grow from small to large size during intensification. The error bars indicate one standard deviation below and above average values.

data, the focus in this section is on the 18 TCs that are categorized as large throughout the intensification period from TS to TY and the 16 TCs that are persistently small in size during intensification (Table 2). In general, both the persistently small and large TCs occur quite evenly over the six years. Given the short period of study, it is beyond the scope of this study to investigate climate factors for interannual variability of TC size.

Comparison of the best tracks of the large and small TCs indicates quite distinguishable track types from the two groups. Almost all of the large TCs developed in the latitude band of 10°–15°N in the WNP monsoon trough area and traveled westward or northwestward during development to TS (Fig. 6a). As verified with 500-hPa geopotential height composites (not shown), these were south of the subtropical high during development to TS, moved to southwest of the high when attaining TS intensity, and then were west of the high when the TY stage was reached. In addition, the tendency for northwestward motion is consistent with a larger northwestward BEP for TCs with a larger outer core wind speed (Carr and Elsberry 1997).

By contrast, the initial positions of the small TCs are more scattered and specifically have a much larger spread in their latitudes of formation (Fig. 6b). These TCs can be roughly divided into two groups: those that formed south of about 15°N and the remainder that formed in higher latitudes. The lower-latitude small TCs formed in the

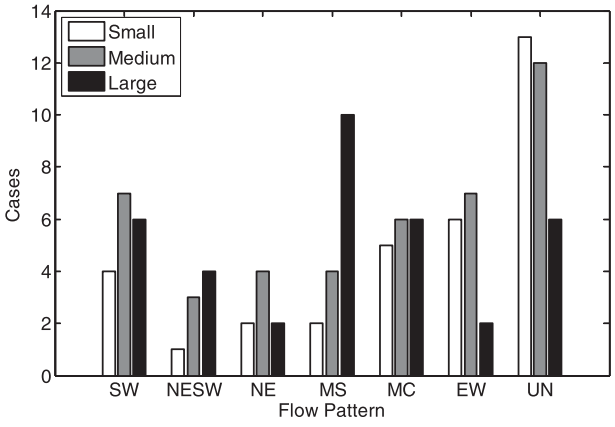

FIG. 7. Histograms of small, medium, and large tropical storms that formed in the six synoptic patterns of easterly wave (EW), southwesterly flow (SW), northeasterly–southwesterly (NESW), northeasterly flow (NE), monsoon shear (MS), and monsoon confluence (MC) as defined by Lee et al. (2008); UN indicates unclassified cases for which no unique flow pattern is identified.

monsoon trough area and migrated west-northwestward following the usual northwest–southeast orientation of the trough. Unlike the tendency of recurvature for the large TCs that form in a similar region, these lower-latitude small TCs generally maintain a similar direction of motion after they attained TY intensity. This track can be interpreted as due to a lack of a contribution from the BEP, which is weaker for small TCs with small outer core strength; also, smaller-size TCs have less capability to cause a weakness in the subtropical ridge (Carr et al. 2001). Further, with stable steering by the easterlies from the subtropical ridge, these westward-moving TCs do not experience much variation in the upper-level eddy flux convergence and vertical wind shear, which is another possible reason why they maintain small size during intensification.

For the small TCs that originate in higher latitudes (Fig. 6b), two move northward and two others move eastward in the South China Sea. Usually, northward motion in higher latitudes is due to breaks in the subtropical ridge. On the other hand, many TCs that originated in the South China Sea move eastward or northeastward following the southwesterly flow in the East Asian monsoon (Fig. 6c). For the four small TCs that have westward tracks, 500-hPa geopotential height composites (not shown) also confirm that they were mostly south of the subtropical high throughout the intensification to TY (Fig. 6c).

b. Synoptic-scale influence on TC size variability during intensification

Composites of the wind fields at various levels and at different times before TS intensity is reached, and at different intensities after the TS stage, are prepared separately for the persistently large and small TC groups. At 72 h before TS intensity, the 18 large TCs

TABLE 2. The 16 small and 18 large TCs that have the same size category for R15-TS and R15-TY (i.e., those cases in the upper left and lower right entries in Table 1). The cases in bold are those that had a nearby TUTT cell during their formations, as discussed in section 5.

	Small TCs				Large TCs			
Year	No.	Name	R15-TS	R15-TY	No.	Name	R15-TS	R15-TY
2000	**13W**	**Jelawat**	**0.8**	**0.9**	15W	Ewiniar	3.7	3.7
	22W	Saomai	1.0	0.6	**20W**	**Prapiroon**	**3.1**	**3.6**
	29W	Yagi	0.7	1.2				
2001	09W	Kongrey	0.9	1.5	06W	Utor	6.7	6.7
	20W	Nari	0.8	0.8	14W	Pabuk	5.7	4.8
	21W	Vipa	0.7	1.0	25W	Haiyan	3.3	3.5
	24W	Krosa	0.7	1.4				
2002	07W	Noguri	0.6	0.9	09W	Rammasun	3.9	4.7
	14W	Fungwong	0.7	1.3	**19W**	**Phanfone**	**3.2**	**3.9**
					21W	Rusa	1.8	2.8
					26W	Bavi	6.7	7.8
					30W	Haishen	2.4	4.5
2003	02W	Kujira	1.1	1.5	11W	Etau	2.2	2.7
	12W	Krovanh	0.7	1.4	16W	Choiwan	2.8	3.0
	15W	Maemi	0.8	1.4	**17W**	**Koppu**	**2.6**	**3.8**
					21W	Parma	2.1	3.1
2004	14W	Meranti	0.5	1.8	11W	Tingting	2.4	4.4
					16W	**Rananim**	**2.7**	**3.9**
					20W	Aere	3.2	3.8
2005	02W	Roke	0.7	0.5	09W	Matsa	2.3	3.9
	04W	Nesat	0.5	0.9				
	11W	Mawar	1.1	1.4				

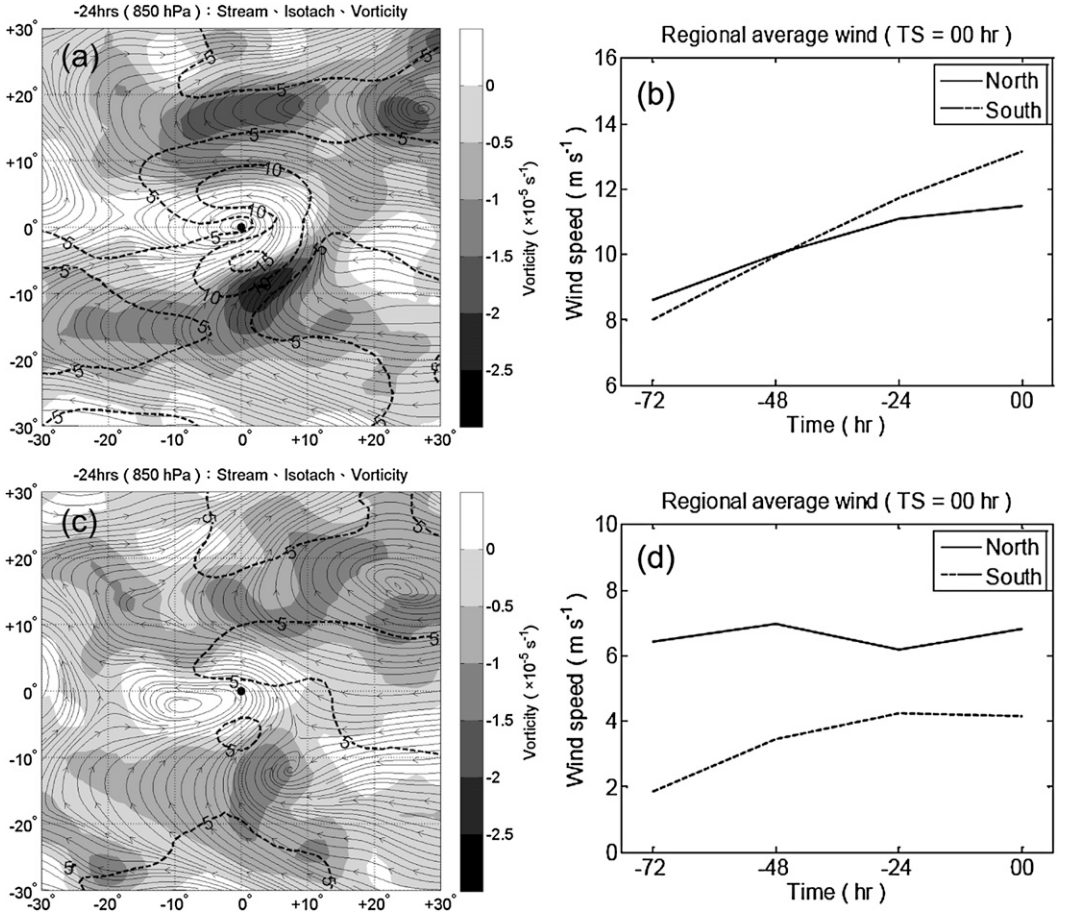

FIG. 8. (a) Composite 850-hPa streamline, wind speeds (dashed lines), and relative vorticity (shaded) 24 h before formation of the 18 persistently large TCs. (b) Average 850-hPa wind speed in a 14° lon × 7° lat region displaced a distance of 3° lat to the north (solid) and to the south (dashed) from 72 h before formation to formation time ($t = 0$) for the 18 persistently large TCs. (c),(d) As in (a),(b), respectively, but for the 12 persistently small TCs that have westward tracks.

were embedded in a strong 850-hPa cyclonic shear environment. The wind speeds just outside the core region both south and north of the center were over 10 m s^{-1} (Fig. 8a). As these storms approached the TS stage, the southwesterly winds south of the TC center increased gradually. Time series of average 850-hPa wind speed were calculated within domains of 14° longitude × 7° latitude that have the southern (northern) boundary 3° north (south) of the TC center. The placement of these two domains is intended to examine environmental wind speeds that are not much affected by the TC core region intensification. Slight modifications of the size of the domains do not significantly alter the average wind speeds and the conclusions below.

For the sample of persistently large TCs, the average 850-hPa wind speeds north and south of TC center increase in a similar manner from 72 h before the TS stage (time 00 h in Fig. 8b). With the more rapid increase in southwesterly winds, the average wind speed south of the TC center surpasses that to the north about 48 h before the TS stage and the average environmental wind speed is as high as 12 m s^{-1} when TS intensity is attained. For the 12 persistently small TCs that have westward tracks, the low-level environment includes strong easterlies north of the TC center (Fig. 8c), which are likely enhanced by the meridional pressure gradient between the developing TC and subtropical high (Fig. 8c). These easterlies in the northern box are about 6 m s^{-1} throughout the 72 h before TS intensity, and the average wind speed of the westerlies in the box south of the TC center is initially quite weak and increases to 4 m s^{-1} (Fig. 8d).

The 500-hPa synoptic-scale wind field evolutions for the persistently large and small TCs are not significantly different. Similarly, no significant differences are found at upper levels between the persistently large and small

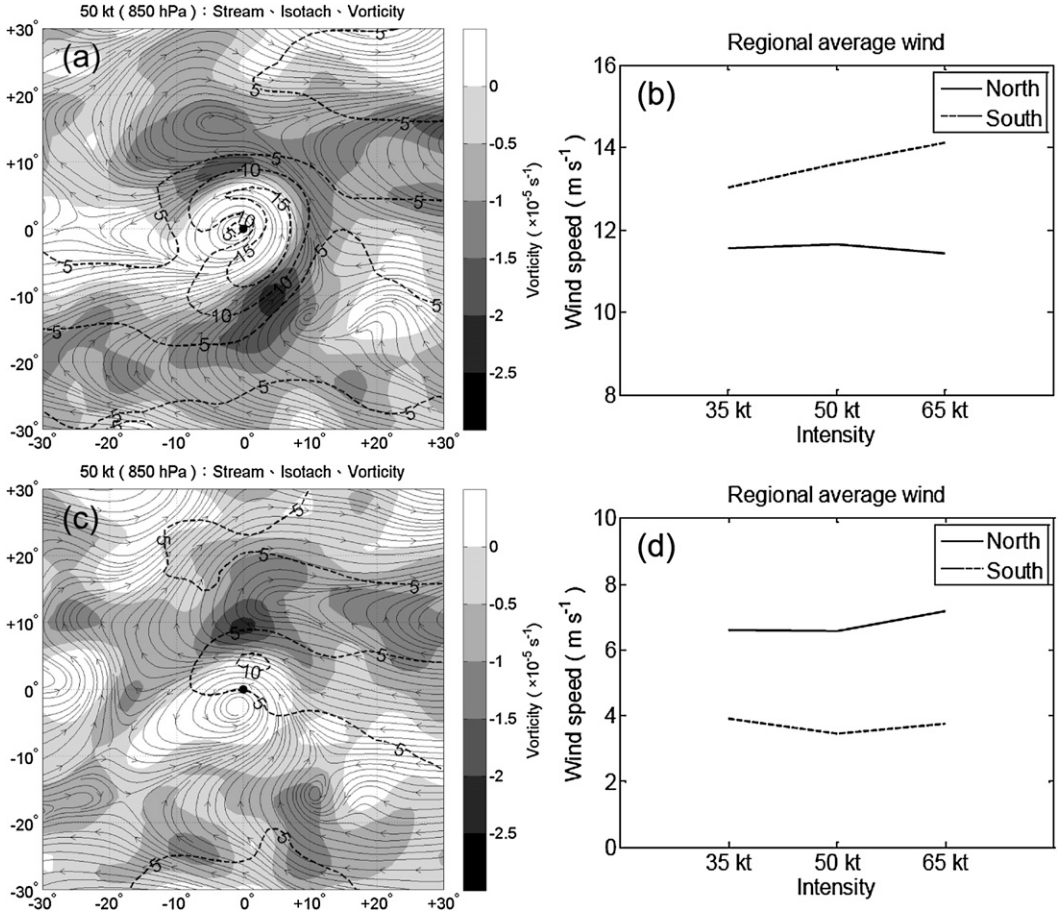

FIG. 9. As in Fig. 8, but the 850-hPa composite streamlines are when the TCs have intensity of 50 kt; (b) and (d) are at various intensities during the intensification stage from TS to TY.

TCs. Thus, the determining factors for TC size evolution are mainly in the lower troposphere.

The JTWC usually issues a TC formation alert (TCFA) for a developing disturbance before it is declared to be a TS. Although the time of issuing a TCFA is quite subjective, it is found that the persistently small TCs only have a TCFA issued 15 h in advance, whereas the average is 26 h for the persistently large TCs. Whereas many small TCs originate in the EW formation pattern and most large TCs originate in the monsoon-related patterns (see section 3d), this difference is consistent with the following findings in Lee et al. (2008). Lee et al. show that on average only a single, short-lived major convection event occurs around 13 h before formation in the EW pattern. By contrast, usually more than one episode of convection or a mesoscale convective system occurs in the monsoon-related patterns prior to formation, which takes around a day before intensifying to TS stage. Thus, these monsoon-related patterns are more favorable for the classic two-stage formation process of Zehr (1992) in which the first deep convection event is followed by a second event when the formation time is approached.

As the persistently large TCs intensify from TS to TY, the region with strongest 850-hPa wind speed is first southeast of center (Fig. 9a) and later extends to regions east and northeast of the center (not shown). This shift of maximum wind speed location may be related to the movement of these large TCs to higher latitudes and to the simultaneous deepening of the central pressure, which tightens the pressure gradient with the subtropical ridge and thus increases the winds in the northeast quadrant of the cyclones. Outside the core region, the low-level wind speeds in the box south of the TC center keep increasing to an average value of about 14 m s^{-1} when TY intensity is attained (Fig. 9b). As in the case of the earlier stage (Fig. 8a), the increase in the southwesterly wind is an important ingredient for establishing and maintaining the size of these large TCs during intensification. By comparison, the average environmental wind speed in the box to the north of center remains almost unchanged during intensification (Fig. 9b).

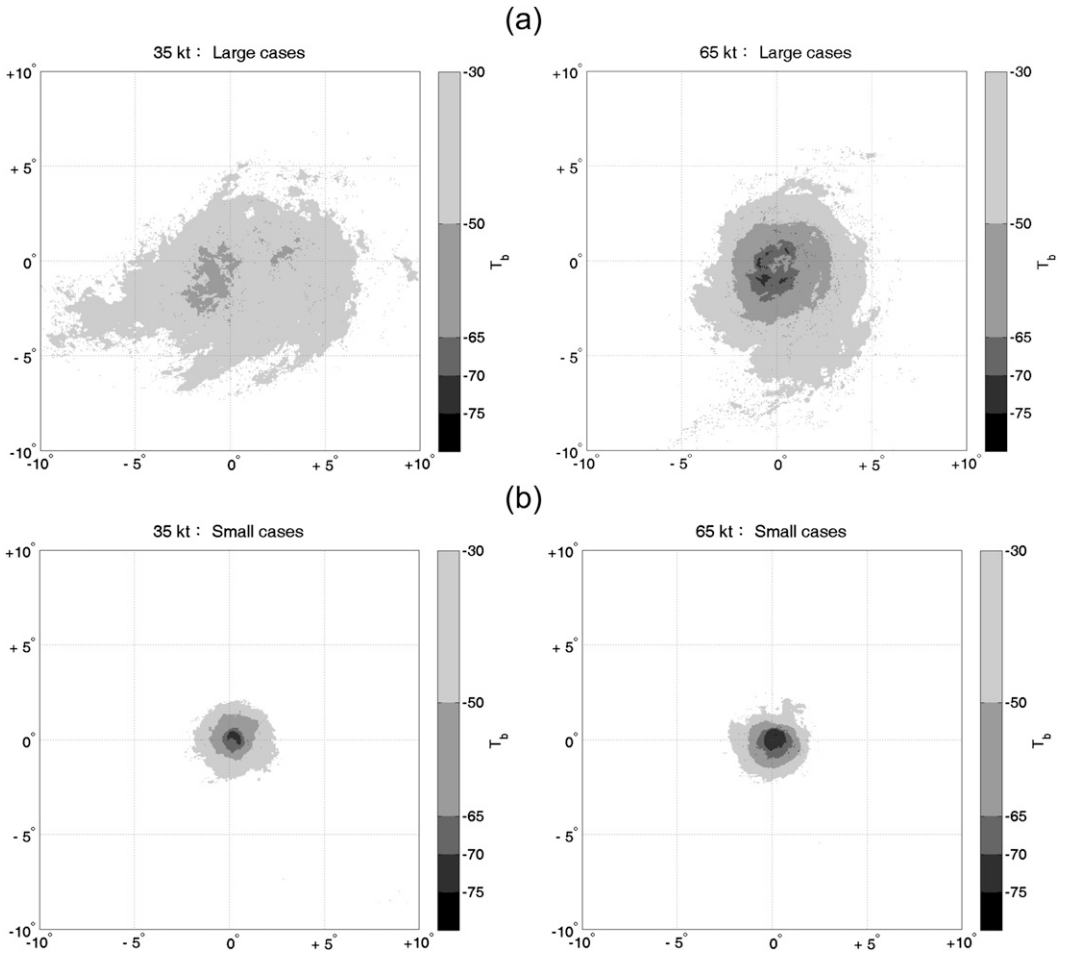

FIG. 10. Composites of cloud-top temperatures lower than −30°C (see scale) for (a) the 18 persistently large TCs and (b) the 16 persistently small TCs at intensities of (left) 35 and (right) 65 kt.

The synoptic situation for the persistently small TCs during intensification is rather similar to that in the early development stage (Fig. 8c) with a dominant subtropical high to the north (Fig. 9c). In this composite, the maximum 850-hPa wind speed is over 10 m s^{-1} about 5° latitude north of the TC center, which again may be due to a tighter pressure gradient between the cyclone and the subtropical high. However, the environmental average wind speed in the box north of the TC center increases only slightly during intensification, and no increase occurs in the box to the south (Fig. 9d). Thus, the environmental wind field evolution for the persistently small TCs is markedly different from the evolution for the large TCs (Fig. 9b). As during the early stage, these changes are confined to the lower troposphere below 500 hPa.

c. *Convection characteristics*

These different low-level synoptic evolutions for the persistently large and small TCs are associated with contrasting convection patterns as well, which is the basis for recognizing TCs with different sizes in satellite imagery. In the composites of the infrared cloud-top temperatures for the persistently large TCs (Fig. 10a), a broad area of convection with radius of about 5° latitude and cloud-top temperature lower than −30°C exists during early stage development. This aerial extent of convection remains similar throughout the period of intensification to TY stage, except that more deep convection develops and consolidates in the inner core region. Notice that the convective activity southeast of the TC just outside a radius of 5° latitude from the center is collocated with the strong southwesterly winds in Fig. 8a. For the persistently small TCs (Fig. 10b), the area with cloud-top temperatures less than −30°C has a radius of only about 2° latitude throughout the intensification period. This compact region of deep convection is fairly symmetric, which suggests that the convection for these small TCs may be less influenced by external environmental factors.

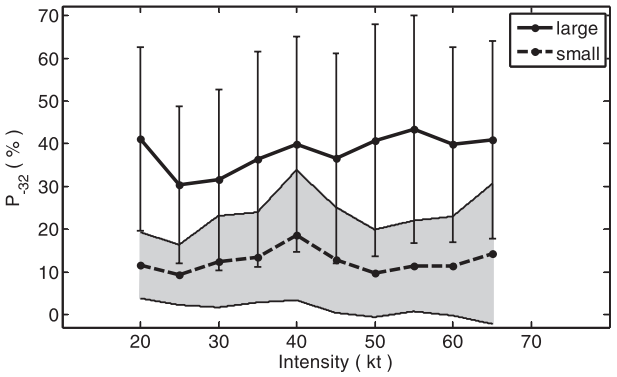

FIG. 11. Average percentage area of convection with cloud-top temperature lower than −32°C computed in a 10° lon × 5° lat region with its northern boundary 5° lat south of TC center for the 18 persistently large (solid) and the 16 persistently small TCs (dashed) as they intensify from 20 to 65 kt. The shaded area and error bars represent one standard deviation below and above the averages.

To quantify the difference in convective activity on the southern side of the persistently large TCs, the percentage of area with cloud-top temperature lower than −32°C (P_{-32}) in an area of 10° longitude × 5° latitude that has its northern boundary 5°S of the TC center is examined. For the persistently large TCs, the portion of this area that has deep convection is between 30% and 40%, and P_{-32} gradually increases from the TS to the TY stage (Fig. 11). For the persistently small TCs, this southern area is almost free of deep convection as P_{-32} is only ~15% throughout the intensification period.

An example of a TC that maintained a large size throughout its development is Typhoon Ewiniar during 2000. On 8 August (Fig. 12a), an extensive area of deep convection existed in a region about 8°–17°N and 138°–145°E. Although the monsoonal cloudiness equatorward of 15°N was even more extensive 36 h later (Fig. 12b), the convection was wrapped around a low-level vorticity center near 23°N, 140°E (Fig. 12c). Although the convection became quite axisymmetric around this system center during the development up to TY intensity, strong convection persisted in extensive north–south bands south and southeast of the center of Typhoon Ewiniar (Figs. 12c,d).

A typical example of a persistently small TC is Typhoon Jelawat, which also developed in 2000. Early development of Jelawat was associated with the EW formation pattern that contained a compact mesoscale convective system near 22°N, 155°E (Figs. 13a,b). The deep convection during the subsequent development of Jelawat (Figs. 13c,d) closely resembles the composite imagery for persistently small TCs in Fig. 10b. Specifically, the deep convection was within a radius of about 2° latitude, and the only other deep convection outside the core region was east of the circulation center and was associated with the easterly wave circulation.

d. Other factors affecting TC size

Besides the climatological factors such as latitude, storm motion, and intensity, some dynamical processes such as eyewall replacement cycles, formation of concentric eyewalls, and formation of annular storms are known to affect TC size. For example, after the eyewall replacement cycle is completed, usually a larger eye results that modifies the inner-to-outer wind structure. When there is a concentric eyewall, a secondary wind maximum will be found in the radial wind profile (Willoughby et al. 1982; Kossin and Sitkowski 2009; Kuo et al. 2009), and again this affects the TC size. The situation is similar in the formation of annular storms although the occurrence frequency is just a few percent of all storms (Knaff et al. 2003, 2008). Since the focus here is more on synoptic system influences on early intensification, the contributions from these dynamical processes to maintenance of TC sizes are not further investigated.

5. Summary and conclusions

a. Summary

In this study, a size parameter, which is defined as the radius of 15 m s^{-1} near-surface wind speed (R15) based on QuikSCAT oceanic winds, is calculated for 145 western North Pacific TCs during 2000–05. Both the seasonal variability and weak dependence on TC intensity of this size parameter are similar to previous studies.

For the 73 TCs that intensified to typhoon intensity during their lifetimes, the 33% and 67% percentiles of R15-TS (size while at tropical storm intensity) and R15-TY (size while at typhoon intensity) are used to categorize small, medium, and large TCs. Most (67% of small, 50% of medium, and 72% of large TCs) of these 73 TCs stay in the same size category during intensification. Although 3 of 24 small tropical storms increase in size to become a large typhoon during intensification, no large tropical storm in this 6-yr database becomes a small typhoon. Many of the small TCs form under the easterly wave (EW) synoptic pattern as defined in Lee et al. (2008). The monsoon-related formation patterns (MC, MS, SW, and NE–SW) of Lee et al. are favorable for forming medium to large tropical storms and typhoons.

While the 18 persistently large TCs from TS to TY stage mostly have northwestward or north-northwestward tracks, the 16 persistently small TCs can be separated into two groups. One group has westward or northwestward

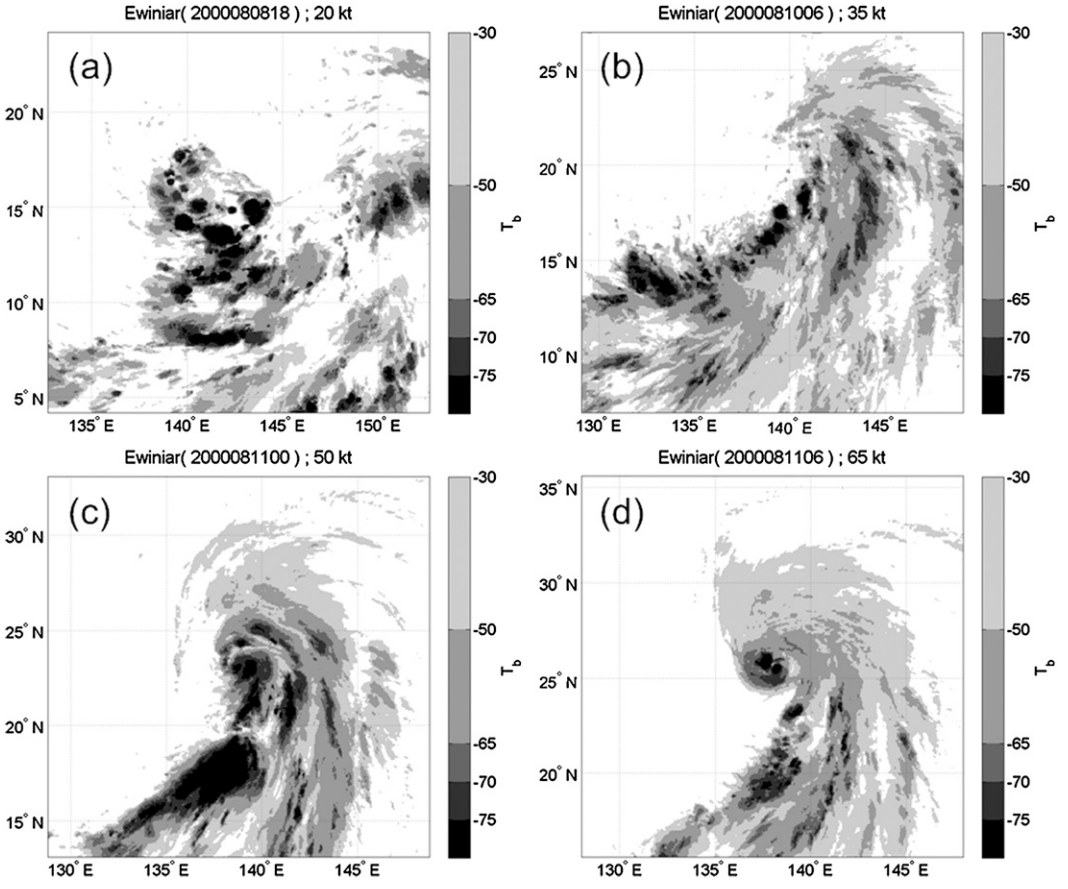

FIG. 12. Enhanced infrared satellite imageries of Typhoon Ewiniar (2000) at (a) 1800 UTC 8 Aug, (b) 0600 UTC 10 Aug, (c) 0000 UTC 11 Aug, and (d) 0600 UTC 11 Aug when the storm had intensities of 20, 35, 50, and 65 kt, respectively.

tracks originating in lower latitudes; another that originates in higher latitudes has both westward- and eastward-moving tracks.

The most distinct synoptic environment feature associated with the persistently large TCs is the strong low-level southwesterly winds that increase gradually from 8 up to 14 m s^{-1} in the outer core (radius $> 3°$ latitude) region south of the TC center throughout the intensification period. These strong southwesterly winds are not present during the intensification of the persistently small TCs, which are more influenced by the subtropical high during intensification. Note that the identification of these strong southwesterlies is not a direct consequence of the definition of large TCs because they are outside the average R15 and thus believed to come from the synoptic environment. Consistent with the differences in synoptic forcing, persistent broad areas of deep convection are present about 5° latitude southwest of the persistently large TC center, but the deep convection with cloud-top temperatures lower than −30°C is usually within a radius of 2° latitude for the persistently small TCs. The deep convection is likely forced by the low-level convergence of the strong southwesterlies and the TC circulation. When the low-level relative vorticity is enhanced through this deep convection, the outer core winds are increased and consequently the R15 is maintained at a large value.

In summary, it is the differences in the environment that determine the differences between persistently large and small TCs directly during formation and indirectly during intensification by its effect on the convection distribution. It should be emphasized that this conclusion is based on examination of low-level flow patterns without consideration of the potential contributions from vertical wind shear and upper-level processes. In addition, the TC size pedigree based on formation patterns as identified here is for the early stage intensification only. Stronger TCs above typhoon intensity can grow in size much more rapidly than the climatological rate under the influence of factors other than those identified in this study.

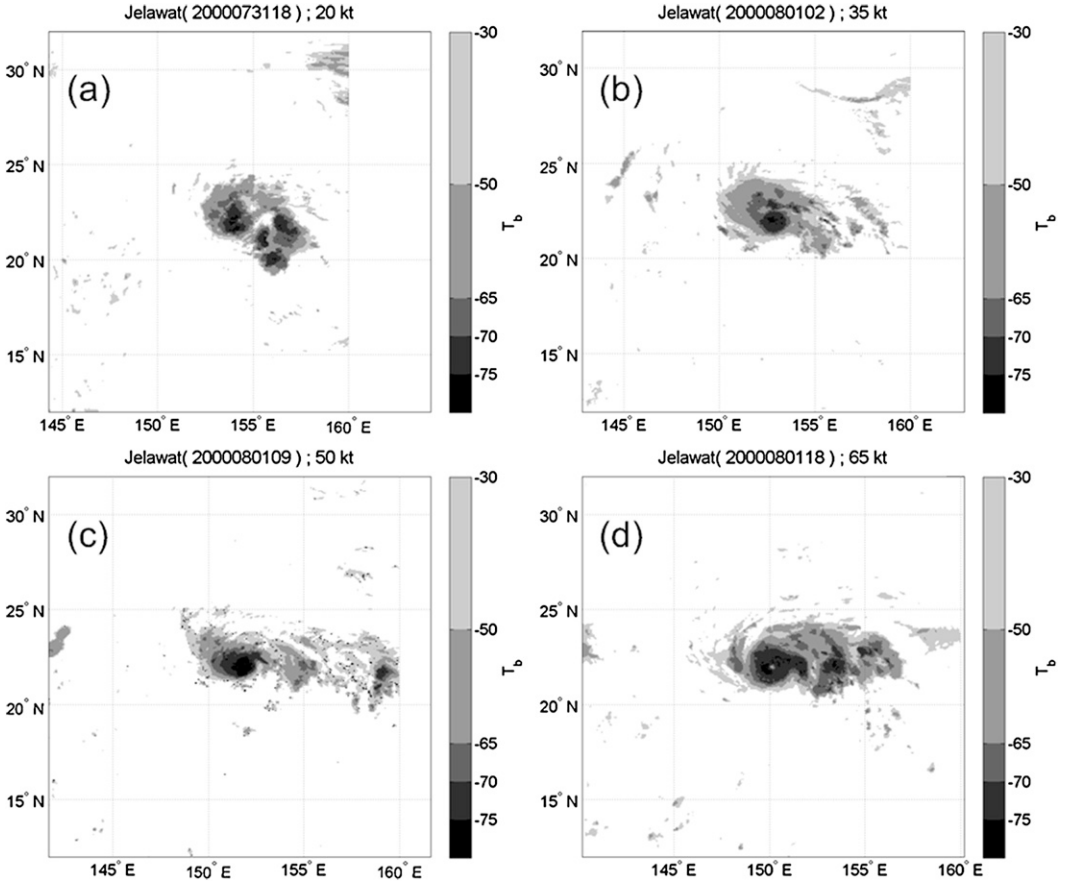

FIG. 13. As in Fig. 12, but for Typhoon Jelawat (2000) at (a) 1800 UTC 31 Jul, (b) 0200 UTC 1 Aug, (c) 0900 UTC 1 Aug, and (d) 1800 UTC 1 Aug.

b. Concluding remarks

Using a vorticity-based size definition, Liu and Chan (2002) found that large TCs were associated with the southwesterly surge and late-season synoptic patterns, while small TCs were associated with dominant subtropical ridge and monsoon gyre synoptic patterns. This study reconfirms that strengthening of the southwesterly winds is as an important ingredient for generating and maintaining large TCs. At least for the northwestward-moving small TCs that originate in low latitudes, the finding in this study that the subtropical ridge to the north has a dominant effect on these small cyclones is again consistent with Liu and Chan (2002). Higher-latitude small TCs that originate in higher latitudes and have quite irregular tracks are likely associated with the tropical upper tropospheric trough (TUTT; Sadler 1976) or have formed from baroclinic systems. This possibility is further explored below.

Hsu (2008) identified certain TC formation cases during 2000–04 that had an upper-level, cold-core low (CCL) in the TUTT located within 10° latitude radius from the system center (termed TUTT-related formation). Some of these cases are classified as persistently small or large TCs in Table 2. Surprisingly, four of the persistently large TCs in this sample are TUTT-related, while only one persistently small case is TUTT-related during its earliest stage of development. The small TC was Typhoon Jelawat (2000) that was discussed in section 4c and illustrated in Fig. 13. Such results would not invalidate the conclusion that most of the persistently small TCs (including Jelawat) form under the easterly wave pattern, and it is this low-level pattern that keeps them small until typhoon intensity. In fact, many cases that Hsu (2008) considered to be TUTT-related are classified in this study as being monsoon-related (because only the low-level synoptic patterns are examined here) including three of the four persistently large TC cases (the other one is unclassified) in Table 2, namely Prapiroon (2000), Koppu (2003), and Rananim (2004). In addition to the low-level forcing as depicted in the earlier analyses, these TUTT-related TCs may also maintain their large size through the environmental forcing mechanisms discussed in Maclay et al. (2008). According to Maclay et al., trough

interaction associated with the TUTT may import additional momentum into the TC core inducing growth. The TUTT may also lead to a more tilted (baroclinic) structure with large vertical wind shear that stimulates convection outside the inner core region and generates asymmetry. The asymmetric heating associated with the convection can then convert baroclinic potential energy into kinetic energy of the TC circulation, and lead to growth in size.

One objective of this study has been to improve understanding of TC size evolution, and ultimately to improve forecasting of TC structure. Knaff et al. (2007) have developed a regression model to establish a TC size climatology as a function of latitude, storm speed, and intensity and then applied a size persistence factor for all TCs in an ocean basin. Some of the findings in this study may be used to improve such a TC structure forecast model. For example, a predictor related to strong low-level southwesterly surges may further improve estimation of the future size evolution of the persistently large TCs. Moreover, developing separate regressions that take into account how the TC size evolution is related to the synoptic patterns at formation as identified here may improve the persistence-type forecast model of Knaff et al. rather than applying the same persistence factor for all TC cases.

Acknowledgments. Comments and suggestions from Dr. John Knaff and the other two anonymous reviewers improved the manuscript substantially, and are much appreciated. This research is supported by the National Science Council and the National Applied Research Laboratories of the Republic of China (Taiwan). The participation of R. Elsberry was funded by the Office of Naval Research Marine Meteorology Division. Mrs. Penny Jones assisted in the manuscript preparation.

REFERENCES

Bessho, K., M. DeMaria, and J. A. Knaff, 2006: Tropical cyclone wind retrievals from the Advanced Microwave Sounding Unit: Application to surface wind analysis. *J. Appl. Meteor. Climatol.,* **45,** 399–415.

Brand, S., 1972: Very large and very small typhoons of the western North Pacific Ocean. *J. Meteor. Soc. Japan,* **50,** 332–341.

Carr, L. E., III, and R. L. Elsberry, 1997: Models of tropical cyclone wind distribution and beta-effect propagation for application to tropical cyclone track forecasting. *Mon. Wea. Rev.,* **125,** 3190–3209.

——, ——, and J. E. Peak, 2001: Beta test of the systematic approach expert system prototype as a tropical cyclone track forecasting aid. *Wea. Forecasting,* **16,** 355–368.

Chan, J. C. L., and C. K. M. Yip, 2003: Interannual variations of tropical cyclone size over the western North Pacific. *Geophys. Res. Lett.,* **30,** 2267, doi:10.1029/2003GL018522.

Cheung, K. K. W., 2004: Large-scale environmental parameters associated with tropical cyclone formations in the western North Pacific. *J. Climate,* **17,** 466–484.

Cocks, S. B., and W. M. Gray, 2002: Variability of the outer wind profiles of western North Pacific typhoons: Classifications and techniques for analysis and forecasting. *Mon. Wea. Rev.,* **130,** 1989–2005.

Demuth, J. L., M. DeMaria, J. A. Knaff, and T. H. Vonder Haar, 2004: Evaluation of Advanced Microwave Sounding Unit tropical cyclone intensity and size estimation algorithms. *J. Appl. Meteor.,* **43,** 282–296.

——, ——, and ——, 2006: Improvement of Advanced Microwave Sounding Unit tropical cyclone intensity and size estimation algorithms. *J. Appl. Meteor. Climatol.,* **45,** 1573–1581.

Ebuchi, N., H. C. Graber, and M. J. Caruso, 2002: Evaluation of wind vectors observed by QuikSCAT/SeaWinds using ocean buoy data. *J. Atmos. Oceanic Technol.,* **19,** 2049–2062.

Elsberry, R. L., and R. A. Stenger, 2008: Advances in understanding of tropical cyclone wind structure changes. *Asia-Pac. J. Atmos. Sci.,* **44,** 11–24.

Fiorino, M., and R. L. Elsberry, 1989: Some aspects of vortex structure related to tropical cyclone motion. *J. Atmos. Sci.,* **46,** 975–990.

Frank, W. M., and W. M. Gray, 1980: Radius and frequency of 15 m s^{-1} (30 kt) winds around tropical cyclones. *J. Appl. Meteor.,* **19,** 219–223.

Hoffman, R. N., S. M. Leidner, J. M. Henderson, R. Atlas, J. V. Ardizzone, and S. C. Bloom, 2003: A two-dimensional variational analysis method for NSCAT ambiguity removal: Methodology, sensitivity, and tuning. *J. Atmos. Oceanic Technol.,* **20,** 585–605.

Holland, G. J., 1983: Tropical cyclone motion: Environmental interaction plus a beta effect. *J. Atmos. Sci.,* **40,** 328–342.

Hsu, K., 2008: An analysis of tropical cyclone formation associated with the upper-level cold-core low (in Chinese; English abstract available.). M.S. thesis, Dept. of Atmospheric Sciences, National Taiwan University, 90 pp.

Kanamitsu, M., W. Ebisuzaki, J. Woollen, S.-K. Yang, J. J. Hnilo, M. Fiorino, and G. L. Potter, 2002: NCEP–DOE AMIP-II reanalysis (R-2). *Bull. Amer. Meteor. Soc.,* **83,** 1631–1643.

Kimball, S. K., and M. S. Mulekar, 2004: A 15-year climatology of North Atlantic tropical cyclones. Part I: Size parameters. *J. Climate,* **17,** 3555–3575.

Knaff, J. A., J. P. Kossin, and M. DeMaria, 2003: Annular hurricanes. *Wea. Forecasting,* **18,** 204–223.

——, C. R. Sampson, M. DeMaria, T. P. Marchok, J. M. Gross, and C. J. McAdie, 2007: Statistical tropical cyclone wind radii prediction using climatology and persistence. *Wea. Forecasting,* **22,** 781–791.

——, T. A. Cram, A. B. Schumacher, J. P. Kossin, and M. DeMaria, 2008: Objective identification of annular hurricanes. *Wea. Forecasting,* **23,** 17–28.

Kossin, J. P., and M. Sitkowski, 2009: An objective model for identifying secondary eyewall formation in hurricanes. *Mon. Wea. Rev.,* **137,** 876–892.

——, J. A. Knaff, H. I. Berger, D. C. Herndon, T. A. Cram, C. S. Velden, R. J. Murnane, and J. D. Hawkins, 2007: Estimating hurricane wind structure in the absence of aircraft reconnaissance. *Wea. Forecasting,* **22,** 89–101.

Kuo, H.-C., C.-P. Chang, Y.-T. Yang, and H.-J. Jiang, 2009: Western North Pacific typhoons with concentric eyewalls. *Mon. Wea. Rev.,* **137,** 3758–3770.

Lander, M. A., A. Zhao, C.-S. Liou, K. Cheung, R. Edson, and J. Franklin, 2006: Operational techniques in defining TC structure. *Proc. Sixth WMO Int. Workshop on Tropical Cyclones,* San José, Costa Rica, WMO, 1.4, 151–159. [Available online at http://severe.worldweather.org/iwtc/.]

Lee, C.-S., K. K. W. Cheung, J. S. N. Hui, and R. L. Elsberry, 2008: Mesoscale features associated with tropical cyclone formations in the western North Pacific. *Mon. Wea. Rev.,* **136,** 2006–2022.

Liu, K. S., and J. C. L. Chan, 1999: Size of tropical cyclones as inferred from ERS-1 and ERS-2 data. *Mon. Wea. Rev.,* **127,** 2992–3001.

——, and ——, 2002: Synoptic flow patterns associated with small and large tropical cyclones over the western North Pacific. *Mon. Wea. Rev.,* **130,** 2134–2142.

Maclay, K. S., M. DeMaria, and T. H. Vonder Haar, 2008: Tropical cyclone inner-core kinetic energy evolution. *Mon. Wea. Rev.,* **136,** 4882–4898.

Merrill, R. T., 1984: A comparison of large and small tropical cyclones. *Mon. Wea. Rev.,* **112,** 1408–1418.

Mueller, K. J., M. DeMaria, J. A. Knaff, J. P. Kossin, and T. H. Vonder Haar, 2006: Objective estimation of tropical cyclone wind structure from infrared satellite data. *Wea. Forecasting,* **21,** 990–1005.

Pickett, M. H., W. Tang, L. K. Rosenfeld, and C. H. Wash, 2003: QuikSCAT satellite comparisons with nearshore buoy wind data off the U.S. West Coast. *J. Atmos. Oceanic Technol.,* **20,** 1869–1879.

Polito, P. S., W. T. Liu, and W. Q. Tang, 2000: Correlation-based interpolation of NSCAT wind data. *J. Atmos. Oceanic Technol.,* **17,** 1128–1138.

Powell, M. D., and T. A. Reinhold, 2007: Tropical cyclone destructive potential by integrated kinetic energy. *Bull. Amer. Meteor. Soc.,* **88,** 513–526.

——, S. H. Houston, L. R. Amat, and N. Morisseau-Leroy, 1998: The HDR real-time hurricane wind analysis system. *J. Wind Eng. Ind. Aerodyn.,* **77–78,** 53–64.

Quilfen, Y., B. Chapron, T. Elfouhaily, K. Katsaros, and J. Tournadre, 1998: Observation of tropical cyclones by high-resolution scatterometry. *J. Geophys. Res.,* **103,** 7767–7786.

Ritchie, E. A., and G. J. Holland, 1999: Large-scale patterns associated with tropical cyclogenesis in the western Pacific. *Mon. Wea. Rev.,* **127,** 2027–2043.

Sadler, J. C., 1976: A role of the tropical upper tropospheric trough in early season typhoon development. *Mon. Wea. Rev.,* **104,** 1266–1278.

Weatherford, C. L., and W. M. Gray, 1988a: Typhoon structure as revealed by aircraft reconnaissance. Part I: Data analysis and climatology. *Mon. Wea. Rev.,* **116,** 1032–1043.

——, and ——, 1988b: Typhoon structure as revealed by aircraft reconnaissance. Part II: Structural variability. *Mon. Wea. Rev.,* **116,** 1044–1056.

Weissman, D. E., M. A. Bourassa, and J. Tongue, 2002: Effects of rain rate and wind magnitude on SeaWinds scatterometer wind speed errors. *J. Atmos. Oceanic Technol.,* **19,** 738–746.

Willoughby, H., J. Clos, and M. Shoreibah, 1982: Concentric eye walls, secondary wind maxima, and the evolution of the hurricane vortex. *J. Atmos. Sci.,* **39,** 395–411.

Yuan, J., D. Wang, Q. Wan, and C. Liu, 2007: A 28-year climatological analysis of size parameters for northwestern Pacific tropical cyclones. *Adv. Atmos. Sci.,* **24,** 24–34.

Zehr, R. M., 1992: Tropical cyclogenesis in the western North Pacific. NOAA Tech. Rep. NESDIS 61, 181 pp.